

Confined-Direct Electric Curing of NaOH-activated fly ash based brick mixtures under free drainage conditions: Part 2. Confined-DEC versus oven curing

Mateusz Ziolkowski^{a*}, Maxim Kovtun^a

^aDepartment of Civil Engineering, University of Pretoria, Pretoria, 0002 South Africa

mateusz.zski@gmail.com (M Ziolkowski)

max.kovtun@up.ac.za (M Kovtun)

*Corresponding author at: Department of Civil Engineering, University of Pretoria, Pretoria, 0002 South Africa. Tel.: +27 78 765 4554. E-mail address: mateusz.zski@gmail.com (M Ziolkowski)

Abstract

A novel accelerated curing technique – confined-DEC (Direct Electric Curing) – was compared with oven curing. Microstructural investigations revealed that under free drainage conditions non-uniform curing conditions were induced within NaOH-activated fly ash based brick mixture during confined-DEC. Strength development of the outer-core (surface) regions of the mixture was impaired by diminished alkali content due to movement of pore solution, resulting in lower compressive strength at later ages compared to identical mixtures cured in an oven for 16 h. Nevertheless, confined-DEC is a promising technique for brick mass production as the requirements of several strength classes of the South African concrete masonry units' standard SANS 1215:2008 were met in 7 min.

Keywords: Alkali-Activated; Fly Ash; Confined-Direct Electric Curing; Acceleration; Brick; Compressive strength; ATR-FTIR; XRD; XRF; TGA.

1. Introduction

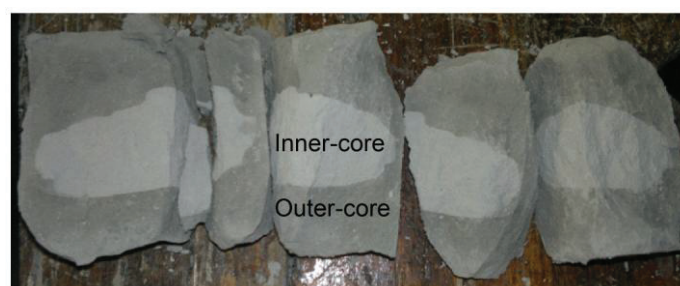
In South Africa where electricity production relies mainly on coal-fired power plants, only 7% of fly ash generated is recycled and the rest, including bottom ash, is stacked in dumps or ash dams, creating landfills [1]. The South African National Development Plan 2030 (NPD), regarded as one of the country's most strategic initiatives, is focused on addressing the waste-to-landfill problem, and one of the strategic objectives is to reduce landfilling by recycling waste [2]. Another NPD priority is to achieve adequate housing and improved living environments, with 1.495 million more households living in new or improved housing conditions by 2019. Taking into account continuously increasing cost of construction materials because of the high demand, scarcity of raw materials and high price of energy, it would be beneficial to develop a low-cost construction material to aid the initiative. Utilisation of alkali-activated fly ash in brick manufacture can be one of the feasible options which would not only help to solve the fly ash storage and environmental issues but also to reduce the exploitation of natural resources. It has been shown that alkali-activated fly ash based bricks could be manufactured by curing at temperatures below 150 °C making the production process significantly less energy intensive in comparison to traditional clay brick production [6, 7]. However, the major drawback of the existing low temperature alkali-activated fly ash brick technologies is the long duration of curing [6, 7]. Under conditions of mass production and rapid turnover in automated plants, a reduction in the curing duration is sought after. Therefore, an alternative accelerated curing technique is needed for mass production of alkali-activated fly ash based bricks.

After considering existing curing techniques and methods used for alkali-activated fly ash materials to accelerate the reaction process, an alternative accelerated curing technique – Confined-Direct Electric Curing (DEC) – was proposed in the Part 1 of the investigation [3]. Detailed literature review on the necessity of an alternative accelerated curing technique, like confined-DEC, for the rapid mass manufacture of fly ash based bricks can be found in the Part 1 [3]. It was shown that the confined-DEC technique was a promising approach in the

rapid accelerated curing of NaOH-activated fly ash based brick mixtures; compressive strength of 11.5 MPa was achieved in 7 min [3]. The confined-DEC technique also supports the mass production of fly ash based bricks on an industrial scale through press moulding [4]. Thus, this concept is a potentially viable alternative solution for high-volume fly ash utilisation.

Although, the Part 1 of the study showed that sufficient compressive strength could be achieved by confined-DEC over a short period of time, the rapid strength development could have adverse effects on the long-term compressive strength of the material due to the removal of pore solution through evaporation process as steam was observed during the application of the confined-DEC [3]. Davidovits and Legrand (1977) [5] observed similar phenomenon when mixture of clay, caustic soda and water was pressed into a mould by a heated up to 150 °C press. The authors reported negative effect of using heated press compared to cold press oven cured mixtures on the bending strength of the final product. Kovalchuk et al. (2007) [8] explain that insufficient amount of water, derived under specific conditions during oven curing, may prevent the glassy component of fly ash from fully dissolving, and thus contribute to loss in potential strength.

Another issue observed with confined-DEC under free drainage conditions was the formation of two distinct regions, inner- and outer-core, within the samples after curing (Fig. 1).



(Single column, 90 mm, fitting image)

Fig. 1. A crushed 50 mm cube immediately after the application of confined-DEC (reproduced from [5]).

It was hypothesized in the Part 1 of the investigation that the formation of these regions was due to the movement of pore solution within the mixture during confined-DEC [3]. When temperature increased during the application of confined-DEC, a hydraulic gradient sufficient for propelling the movement of the pore solution from within the central region to the drainage paths was raised resulting in generation of steam leaving the confined-DEC device. The diminished pore solution prevented further temperature rise (Joule heating) in the outer-core region, creating two distinct regions.

The aim of this part of the investigation is to address the issues observed during confined-DEC in the Part 1 [3]. To evaluate possible adverse effects of confined-DEC, strength development of a NaOH-activated fly ash based brick mixture prepared with confined-DEC was compared to identical mixtures prepared with oven curing. Microstructural investigations were carried out to provide insight into the key differences in the development of the microstructure and mineralogy of mixtures prepared with confined-DEC and oven curing. The standard compliance, South African concrete masonry units' standard (SANS 1215:2008) [9], of samples prepared with confined-DEC was also included in this study.

2. Experimental procedure and material properties

2.1. Experimental set-up

For safety reasons, the design of the confined-DEC set-up was based on the design of Davidovits and Legrand (1977) [7] with regards to relieving the internal water pressure build-up during curing; the compressed material was allowed a capillarity migration of pore solution (free drainage conditions). This prevents dangerous steam outbursts when the confining pressure is removed after curing. Otherwise, in a closed system (un-drained conditions), time must be allowed for the mixture to cool down to a safe temperature before

the mould can be opened, though this would increase the total curing duration. The confined-DEC set-up was designed to produce three 50 mm cubes, in order to obtain statistically significant results in compressive strength development. A detailed description of the confined-DEC set-up can be found in Part 1 of the investigation [3].

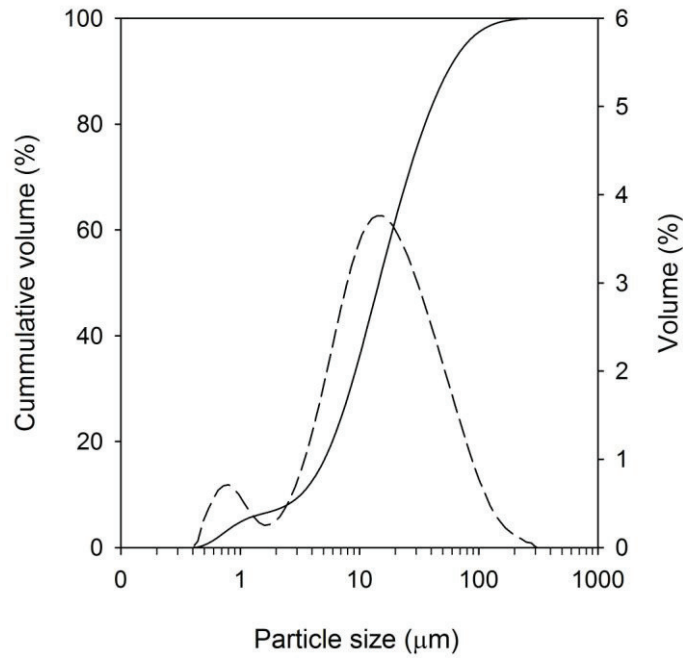
2.2. Materials

A classified fly ash with average density of 2240 kg/m³ and Blaine fineness of 316 m²/kg was used throughout the investigation. The classified fly ash complies with the chemical and physical requirements of BS EN450, ASTM C618 and all relevant international quality standards for fly ash. The chemical composition of fly ash is shown in Table 1. The particle size distribution of the fly ash is depicted in Fig. 2. Commercially available NaOH flakes (98.0 % purity) and tap water were used to prepare NaOH solutions.

Table 1

Chemical composition of fly ash (weight %)

SiO ₂	Al ₂ O ₃	CaO	Fe ₂ O ₃	TiO ₂	MgO	K ₂ O	P ₂ O ₅	Other	LOI
54.9	31.5	4.5	3.5	1.6	1.0	0.8	0.4	0.3	1.0



(Single column, 90 mm, fitting image)

Fig. 2. Particle size distribution of the fly ash

2.3. Mixture preparation

The mixture design of the NaOH-activated fly ash based brick mixture was composed of two parts: binder and aggregate. The binder consisted of fly ash, water and NaOH flakes. For high utilisation of fly ash, the aggregate part consisted of fly ash alone. The mixture design that produced the best compressive strength development with the application of confined-DEC in the Part 1, consisting of 4.1% NaOH flakes, 9% water and 86.9% fly ash by weight (E16, Table 3, [3]), was used throughout this part of the study. The molarity of the NaOH solution was 16.9 mol/l and the mass ratio of the NaOH solution to the total fly ash was 0.151. The detailed mixture design and preparation procedures are presented in the Part 1 [3].

2.4. Sample preparation

Samples prepared with confined-DEC were subjected to a confining pressure of 10 MPa and a voltage gradient of 0.8 V/mm (E16, Table 3, [3]). Duration of curing for the confined-DEC samples was based on utilising the full potential of the mixture's Joule heating capability in the shortest possible time and took approximately 7 min. A detailed description of the curing process is presented in the Part 1 [3]. Once the curing was finished, samples were removed from the confined-DEC device and stored at 25 ± 2 °C and $55 \pm 5\%$ relative humidity until testing.

For oven curing, samples were compacted at the same pressure of 10 MPa. After the compaction, samples were dry cured in an oven. Samples were not wrapped in plastic film to replicate a possible real production scenario when “green” bricks would be stacked on a pallet and placed into an oven for curing.

To accelerate the alkali activation process at an observable rate without adverse effects at later ages, Swanepoel and Strydom (2002) [10] concluded that 48 h of oven curing at 60 °C was the optimum curing duration. However, Shekhovtsova et al. (2014) [11], who used fly ash from the same power plant as that used in this investigation, found that the optimum curing duration was 16 h at 60 °C. The difference in optimum duration of curing could be attributed to differences in the alkali activators used in the studies. Swanepoel and Strydom (2002) [10] used a mixture of NaOH and Na₂SiO₃, and Shekhovtsova et al. (2014) [11] used sole NaOH. Shekhovtsova et al. (2014) [11] found that NaOH-activated fly ash binders cured at elevated temperatures of 60 and 80 °C showed small differences in mechanical strength development at 91 days. However, they found that prolong curing at 80 °C resulted in strength decline at 28 and 91 days. Noushini and Castel (2016) [12] observed strength decline in samples exposed to prolong periods at an elevated temperature of 90 °C. Arioz et al. (2012) [13] also found strength reduction of geopolymer samples subjected to a high elevated curing temperature of 120 °C. Van Jaarsveld et al. (2002) [14] observed that rapid curing and/or curing at too high temperatures resulted in cracking and thus had a negative effect on the

physical properties of the samples. Two temperatures, 60 and 90 °C, were therefore chosen for this investigation. The 60 °C curing regime was employed as a control since it did not have detrimental effects on strength development at later ages. A 90 °C oven curing regime was also included to provide a comparison to samples exposed to a curing environment that would possibly have detrimental effects on the strength. The duration of both oven curing regimes was limited to 16 h [11]. After curing, samples were stored at 25±2 °C and 55±5% relative humidity until testing.

2.5. Comparison analysis procedure

To understand effects of confined-DEC on development of the NaOH-activated fly ash based brick mixture, a comparison was made between samples prepared with confined-DEC and the two oven curing regimes. The comparison focused on compressive strength development and assessment of microstructural differences between the samples.

Attenuated total reflection Fourier-transform infrared spectroscopy (ATR-FTIR), X-ray diffraction (XRD), X-ray fluorescence (XRF) and thermal gravimetric analyses (TGA) were used to evaluate the microstructural and mineralogical evolution over time and the differences between samples subjected to the three curing regimes. The analyses also provided insight into the changes in microstructure responsible for compressive strength development of the samples. Table 2 presents the time of analysis for each test.

Table 2

Time and type of analysis

Time of analysis	Curing regime		
	Confined-DEC	Oven-cured-60 °C	Oven-cured-90 °C
Right after curing	Compressive strength test, ATR-FTIR and XRD	-	-

1 day	Compressive strength test, ATR-FTIR, XRD and TGA	Compressive strength test, ATR-FTIR, XRD and TGA	Compressive strength test, ATR-FTIR, XRD and TGA
7 days	Compressive strength test	Compressive strength test	Compressive strength test
28 days	Compressive strength test, ATR-FTIR, XRD and XRF	Compressive strength test, ATR-FTIR and XRD	Compressive strength test, ATR-FTIR and XRD

During compressive strength testing, samples were crushed at a rate of 15 MPa/min, as prescribed by the South African concrete masonry units' standard (SANS 1215:2008) [9]. Three 50 mm cubes were tested at each age. Average of the results was reported as compressive strength value. After cubes were crushed on their respective days of analysis, samples for the characterisation techniques were randomly collected and then dehydrated to prevent further material evolution. To avoid alteration of the binder gel and pore structures as a result of the drying process, the recommended dehydration method by Ismail et al. (2013) [15] was used. The crushed samples were dehydrated by submerging them in acetone for 15 min and then filtering them using a vacuum pump. After dehydration, the samples were sealed in a tube until analysis. Each characterisation technique was performed once.

The samples for XRD analysis were prepared using a back-loading preparation method. The Rietveld method was included as part of the quantitative XRD analysis to indirectly determine the amorphous content of the samples. Determination of the amorphous content involved the addition of 20% Si (Aldrich 99% pure) by weight to ground samples. Mixtures of the samples with crystalline Si were micronized in a McCrone mill with alcohol. The prepared samples were then analysed using a PANalytical X'Pert PRO powder diffractometer with an X'Celerator detector, variable divergence and fixed receiving slits, with Fe filtered Co-K α radiation ($\lambda = 1.789 \text{ \AA}$). The data were recorded in the angular range $5^\circ < 2\theta < 90^\circ$. The phases were identified using X'Pert Highscore Plus software. The relative phase amounts (weight %) were estimated using the Rietveld method (AutoQuan software) within a 3 sigma level of error.

ATR-FTIR of the samples was recorded on a solid state by a VERTEX 70v spectrometer equipped with the Golden Gate diamond ATR cell (Bruker). ATR-FTIR data were recorded on the 4000–400 cm^{-1} spectral region, with 32 acquisitions at a 4 cm^{-1} resolution.

TGA of samples was carried out using a Thermal Analyzer Instrument SDT-Q600. The samples were heated from 30 to 1200 °C at a heating rate of 20 °C/min, under a 100 $\text{m}\ell/\text{min}$ nitrogen purge.

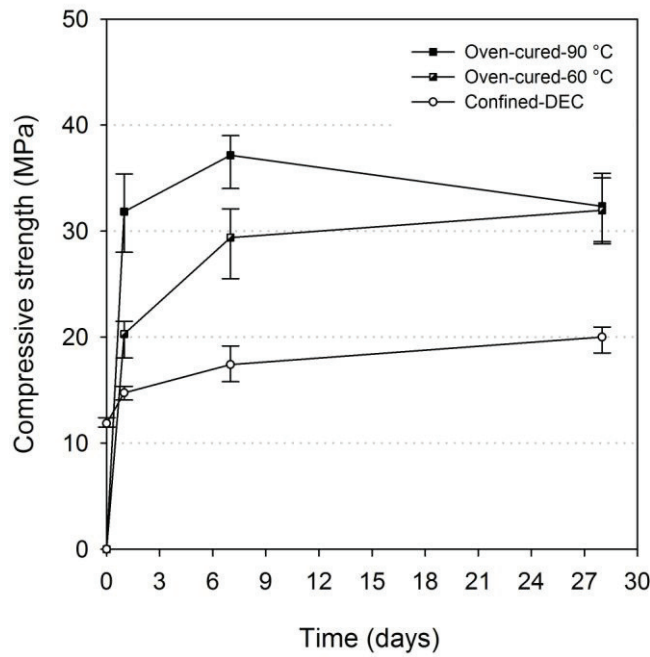
The characterisation techniques were applied to the centre of the oven-cured samples. However, two distinct regions, the inner- and outer-core, were observed in the confined-DEC samples right after the samples were crushed (Fig. 1). The inner-core formed in the centre of 50 mm cube samples. The outer-core was the surface part of the samples. To elucidate any microstructural and mineralogical differences between these two regions, the characterisation techniques for the confined-DEC samples were applied to both regions. Great care was taken during sampling to get a representative specimen of each region.

In addition, XRF of the inner- and outer-core was performed at 28 days to provide supportive evidence for the mechanism of the formation of these regions. The ARL Perform'X Sequential XRF instrument with Uniquant software was used for XRF analyses. The values were normalised, as no loss of ignition was done to determine crystal water and oxidation state changes.

3. Results and discussion

3.1 Compressive strength development

The compressive strength development of the NaOH-activated fly ash based brick mixture prepared with the three different curing regimes is shown in Fig. 3.



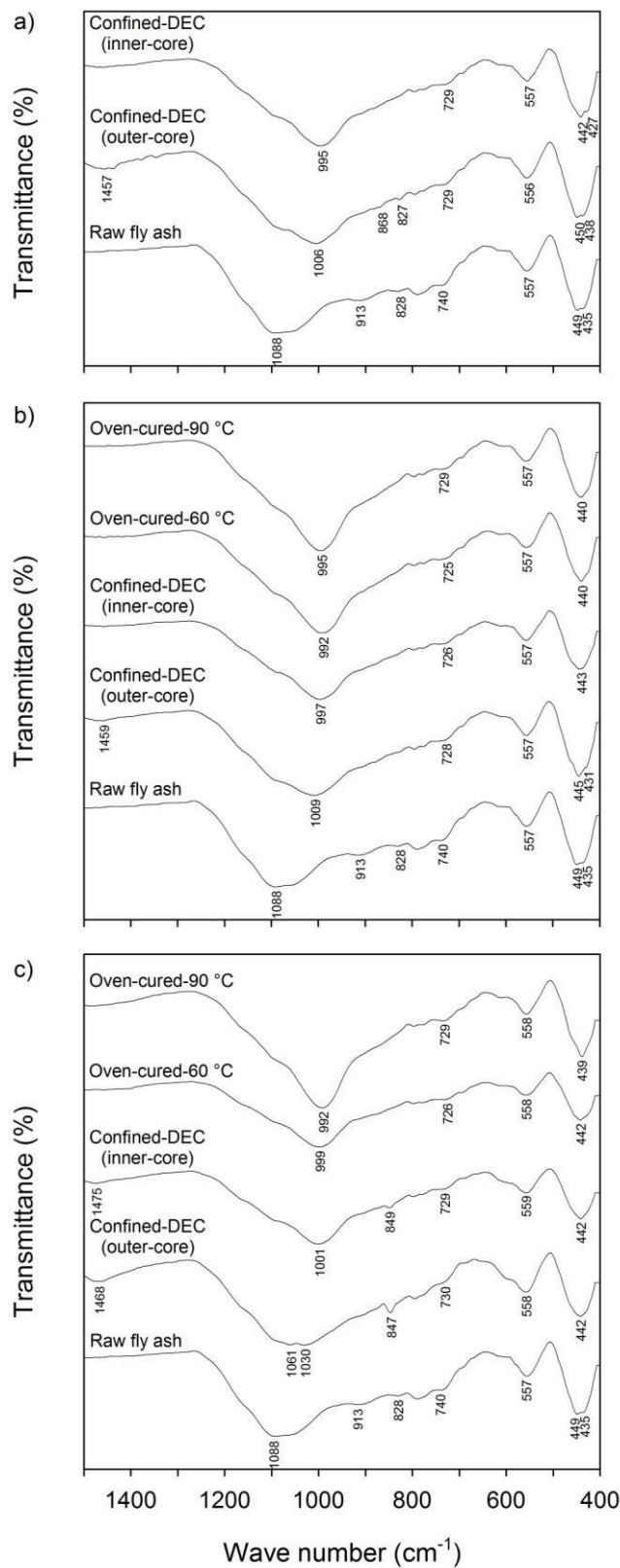
(Single column, 90 mm, fitting image)

Fig. 3. Compressive strength development of samples subjected to different curing regimes

After approximately 7 min of curing with confined-DEC, the samples acquired an average compressive strength of 11.5 MPa. The confined-DEC samples continued to increase in compressive strength after curing, but at a lower rate in comparison to oven-cured samples, reaching an average compressive strength of 20.1 MPa at 28 days. From 1 to 28 days, the compressive strength development of samples prepared with both oven curing regimes resulted in higher compressive strengths than that of the confined-DEC samples. The strength decline at 28 days of 90 °C oven-cured samples is attributed to excessive moisture evaporation during curing [11]. Prolonged curing at elevated temperatures breaks down the gel structure of the geopolymer, resulting in dehydration and excessive shrinkage as the gel contracts without transforming to a more semi-crystalline structure [14]. The confined-DEC samples did not show any strength loss at 28 days suggesting that steam observed during confined-DEC [3] did not cause excessive dehydration. Although the confined-DEC technique produced substantial compressive strength within 7 min, at 28 days the percentage gain difference was 40% lower than for the oven-cured samples.

3.2. Attenuated total reflection Fourier-transform infrared spectroscopy

The ATR-FTIR spectra from 1500 to 400 cm^{-1} of the oven-cured samples and the inner- and outer-core of the confined-DEC samples are presented in Fig. 4.



(Single column, 90 mm, fitting image)

Fig. 4. ATR-FTIR of samples a) right after curing, b) at 1 day and c) at 28 days

The ATR-FTIR of all samples between 4000 and 1500 cm^{-1} (not shown in Fig. 4) did not present any significant differences at all ages. Stretching and deformation of water molecules were detected at 3450 and 1640 cm^{-1} , respectively, in the oven-cured samples and in the inner-core of the confined-DEC samples. This suggests that the induced drying method might not completely have removed water. However, Ismail et al. (2013) [15] explain that this is due to the presence of chemically bound water in the alkali aluminosilicate gel.

The main band in the raw fly ash, 1088 cm^{-1} , was associated with the T-O (where T = Si or Al) asymmetric stretching vibrations [16]. The shift in the main band for samples at all ages was attributed to the formation of alkali aluminosilicate gel as a result of NaOH activation [18]. The position of the band varied between samples prepared with different curing regimes. The T-O band shifted to 992 and 995 cm^{-1} for samples oven-cured at 60 and 90 °C, respectively, at 1 day. From 1 to 28 days, the T-O band for 60 °C samples shifted back to a higher frequency of 999 cm^{-1} . This pendulum movement was due to the consecutive formation of two gels: an Al-rich gel which subsequently evolved into a Si-rich gel, improving the mechanical properties of the material [18]. However, for samples cured at 90 °C, the band did not revert but resulted in an even lower frequency of 992 cm^{-1} . It was probably due to excessive dehydration preventing the reversion of the associated band of the T-O, which also coincided with a slight decrease in compressive strength development at 28 days (Fig. 3).

The T-O band of the inner-core of confined-DEC samples shifted to 995 cm^{-1} after curing and reverted to 997 and 1001 cm^{-1} at the ages of 1 and 28 days, respectively. In the outer-core of confined-DEC samples, the same movement was observed: The band shifted to 1006 cm^{-1} after curing and reverted to 1009 and 1030 cm^{-1} at the ages of 1 and 28 days, respectively. The pendulum movement of the band corresponded to the compressive strength development of the confined-DEC samples (Fig. 3). This also indicates that if the relationship between excessive dehydration from curing and the non-reversion of the band holds true, then

excessive dehydration did not occur in the inner-core of the samples even though steam was observed during confined-DEC.

The bands at 913 and 830 cm^{-1} , present in the raw fly ash, disappeared at all ages in both oven-cured samples and in the inner-core of the confined-DEC samples. Shekhovtsova (2015) [19] also observed the disappearance of these two bands after samples were subjected to oven curing. This was not the case in the outer-core of the confined-DEC samples right after curing: the band at 913 cm^{-1} disappeared, but the band at 827 cm^{-1} was still present. This indicates that the outer-core was not exposed to a curing environment similar to that of the inner-core. However, this band for the outer-core disappeared at a later age, indicating that alkali activation had proceeded, but at a slower rate.

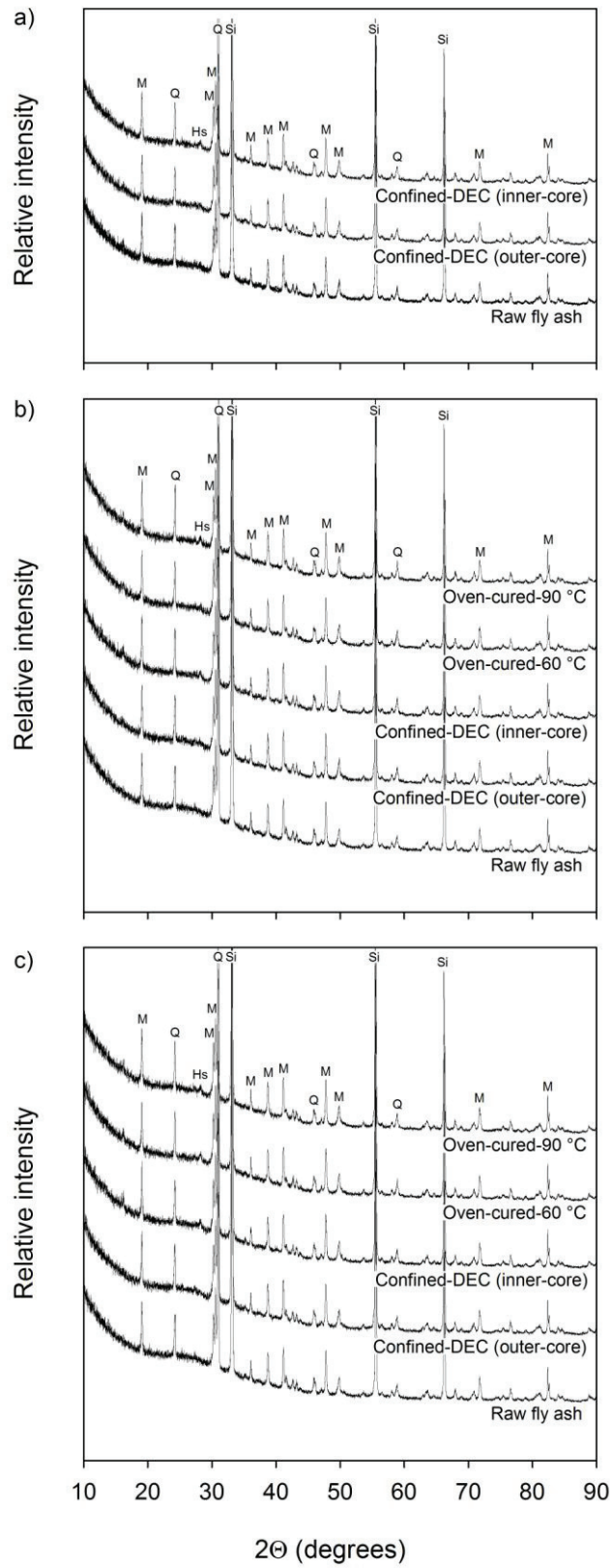
At 28 days, a new band appeared at 847 and 849 cm^{-1} for the outer- and inner-core, respectively. This band was more intense for the outer-core than for the inner-core. Zhang et al. (2009) [20] explain that the band at approximately 840 cm^{-1} can be assigned to the bending vibration of Si-OH. This can be caused by some bond breakage sites in the network structure of the geopolymer; and Zhang et al. (2009) [20] further explain that the presence of Si-OH would cause a decrease in the degree of condensation and, thus, a reduction in mechanical strength development. This corresponded with the lower compressive strength development of the confined-DEC samples at the age of 28 days (Fig. 3). The oven-cured samples did not possess this band and, therefore, had higher compressive strength development. Shekhovtsova (2015) [19] also observed this association: a band at 848 cm^{-1} was found for samples cured at 25 °C and resulted in lower strengths than in samples oven-cured at 40 and 60 °C, which did not possess this band. In this study, the confined-DEC samples have reached 60 °C during curing [3]. Thus, the main reason, why the breakage happened in the confined-DEC samples, was not the temperature but rather duration of curing at elevated temperature which was only 7 min in comparison to 16 h for the oven-cured samples.

The O-C-O stretching vibration band in the region between 1410 and 1570 cm^{-1} was associated with atmospheric carbonation [21]. The sodium present in the samples reacted with CO_2 from the atmosphere. Even after a brief exposure to the atmosphere, between removing the samples from the confined-DEC device to crushing and finally preserving them, the band had already appeared in the outer-core sample. Criado et al. (2005) [22] explain that during the early stages of the process, when the material is in contact with the atmosphere, carbonation occurs rapidly. Due to the highly basic nature of the material, there is a strong thermodynamic tendency to reduce the pH. Criado et al. (2005) [22] further indicate that, as the material becomes more compact due to an increase in the degree of reaction, it becomes more difficult for CO_2 to penetrate the matrix, explaining why the band in the inner-core only appeared at 28 days. Neither of the oven-cured samples possessed this band for all ages. This indicates that the oven-cured samples developed a more compact matrix than did the confined-DEC samples.

In summary, the outer-core experienced a different curing environment to that of the inner-core of the confined-DEC samples. This is in agreement with Part 1 of the investigation [3].

3.2. X-ray diffraction and fluorescence

The XRD patterns of the studied samples are shown in Fig. 5.



(Single column, 90 mm, fitting image)

Fig. 5. XRD patterns of samples a) right after curing, b) at 1 day and c) at 28 days; M: mullite; Q: quartz; Hs: hydrosodalite

The results of XRD analysis revealed that the predominant crystalline phases for all samples, which were also found in the raw fly ash, were mullite and quartz. XRD analysis indicates that, irrespective of the curing method or the day of analysis of the samples, the crystalline phases of the samples were not significantly altered from the raw fly ash. However, a new peak appeared around $28^\circ 2\theta$ for the oven-cured samples and the inner-core of the confined-DEC samples at all ages. Shekhovtsova (2015) [19] also observed this peak and associated it with the zeolite structure hydrosodalite; the author observed that the peak's intensity increased with an increase in Na_2O content. Hence, the intensity of the peak should be the same throughout the confined-DEC samples at all ages. However, this was not the case in the present study. The inner-core of the confined-DEC samples acquired a noticeable peak at all ages, whereas the outer-core did not. This suggests that the outer-core did not experience the same curing environment as that of the inner-core during confined-DEC, supporting the physical observations in the Part 1 of the investigation [3] and the ATR-FTIR results.

Although the crystalline phases were not significantly altered, the compressive strength development of the studied samples differed substantially at all ages (Fig. 3). Van Jaarsveld et al. (2002) [14] explain that the changes responsible for the differences in samples' compressive strength originate from and take place within the amorphous part of the structure and not the crystalline phases. The total amorphous phase content of an alkali-activated material is the combination of the unreacted glassy content in the fly ash and the amorphous reaction product (alkali aluminosilicate gel), where only the amorphous reaction product relates to compressive strength [23]; an increase in amorphous reaction product coincides with an increase in compressive strength. Relative amounts of amorphous phase in the investigated samples are presented in Table 3.

Table 3

Rietveld quantitative results of the amorphous phase contents (weight %)

Age	Fly ash*	Confined-DEC		Oven-cured-60 °C	Oven-cured-90 °C
		Outer-core	Inner-core		
	61.26 ± 0.78				
Right after curing		60.91 ± 0.99	57.68 ± 1.08	-	-
1 day		60.57 ± 0.99	60.91 ± 0.99	58.56 ± 1.05	59.26 ± 0.99
28 days		62.85 ± 0.72	63.99 ± 0.72	64.98 ± 0.69	63.38 ± 0.72

* - the amorphous phase content of the raw fly ash

The relationship between compressive strength development and amorphous phase content holds true for the oven-cured samples. Between 1 and 28 days, an increase in the amorphous phase content coincided with an increase in compressive strength for samples of both oven curing regimes. The amorphous phase content was lower for the 90 °C samples than for the 60 °C samples at 28 days; this was probably due to the excessive moisture evaporation during curing, which also coincided with the drop in strength of the 90 °C samples (Fig. 3).

The relationship between the amorphous phase content and compressive strength does not hold true for the outer-core of the confined-DEC samples. The amorphous phase content of the outer-core right after curing indicates that a considerable increase in amorphous phase content occurred but the compressive strength development did not support this interpretation (Fig. 3). The most plausible scenario is the egress of Na⁺ and OH⁻ ions from the outer-core during confined-DEC, which systematically increased the amorphous phase content (unreacted) of the sample. Considering the initially mixed NaOH-activated fly ash based brick mixture and not just the raw fly ash, the amorphous phase content was adjusted with Equation (1) [24].

$$Ms = p_m \cdot \frac{m_f}{m_f + m_a} \quad (1)$$

where Ms – amorphous phase content of the mixture (%);

p_m – amorphous phase content of the raw fly ash (%);

m_f – mass of the raw fly ash (g);

m_a – mass of the solids of the alkali activator, NaOH (g).

The adjusted amorphous phase content of the studied NaOH-activated fly ash based brick mixture was approximately 58.5%. According to Equation (1), when the amorphous phase content of the raw fly ash is kept constant, the amorphous phase content of the mixture systematically increases with a decrease in NaOH solids. Ahmari & Zhang (2012) [25] explain that during compaction of a mixture, the movement of water out of the mixture leads to the squeezing out of Na^+ and OH^- ions. Hence, the egress of Na^+ and OH^- ions from the outer-core into the drainage path under the action of expansive forces is possible, either in a liquid or gas phase or a combination of both, originating from the centre of the mixture pushing outwards. As mentioned earlier, Shekhovtsova (2015) [19] observed a relationship between Na_2O content and the relative intensity of the hydrosodalite peak; the peak intensity of hydrosodalite increased with increasing Na_2O content. This also supports the argument of the egress of Na^+ and OH^- ions from the outer-core during confined-DEC. A less intense peak for hydrosodalite is expected for samples with a lower Na_2O content; this is in agreement with the XRD results for the outer-core in comparison to the inner-core for all ages (Fig. 5).

Shekhovtsova (2015) [19] also observed that an increase in Na_2O content resulted in an increase in the amorphous phase content. The change in amorphous phase content from right after curing to 28 days was greater for the inner-core ($\approx 6.3\%$) than for the outer-core ($\approx 1.9\%$); this indicates that the total Na_2O content right after the application of confined-DEC in the outer-core sample was considerably less than in the other samples. This further supports the egress of Na^+ and OH^- ions.

The oxide composition of the inner- and outer-core at 28 days is shown in Table 4. The biggest difference in the oxide composition, in weight %, between the outer- and inner-core was attributed to Na_2O content. The Na_2O content in the outer-core was considerably lower

($\approx 20\%$) than that in the inner-core. The XRF results confirmed the egress of Na^+ and OH^- ions from the outer-core during the application of confined-DEC.

Table 4

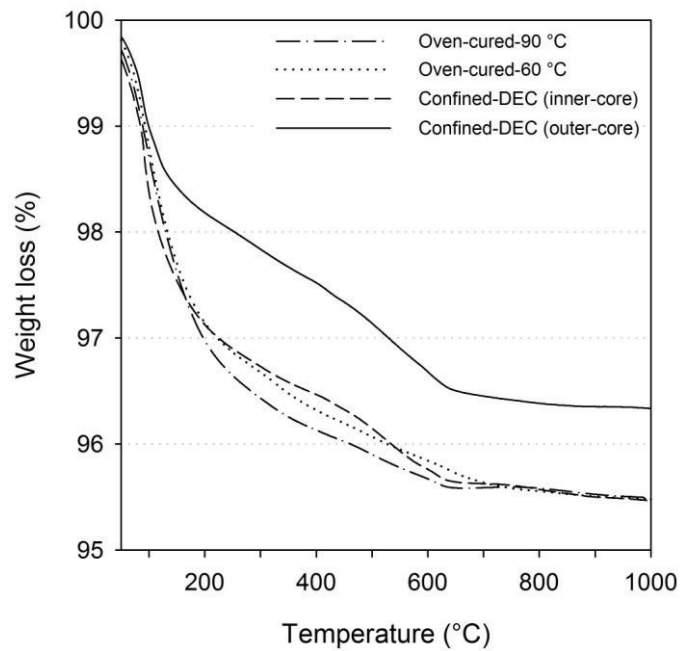
XRF of the inner- and outer-core at 28 days (weight %)

Oxides	Outer-core	Inner-core	% Δ
SiO_2	51.4	50.8	1.2
Al_2O_3	31.1	30.5	2.0
Na_2O	5.7	7.1	-19.7
Other	11.7	11.6	0.9

The movement of the pore solution in the outer-core also means that there was movement of the pore solution in the inner-core. However, the amorphous phase content of the inner-core did not support the egress of ions from the inner-core to the same degree as from the outer-core. The amorphous phase content of the inner-core increased in the period from right after curing to 1 day (Table 3), which indicates that the formation of the alkali aluminosilicate gel was still taking place [23]. Significantly higher increase in the amorphous content in the inner-core from right after curing to 28 days in comparison to the outer-core could also be attributed to higher temperature in the inner-core. The heat generated during confined-DEC was trapped in the inner-core for longer period of time as the outer-core cooled first [3].

3.3. Thermal gravimetric analysis

TGA of the inner- and outer-core of the confined-DEC samples and both oven-cured samples is presented in Fig. 6.



(Single column, 90 mm, fitting image)

Fig. 6. TGA of the samples at 1 day

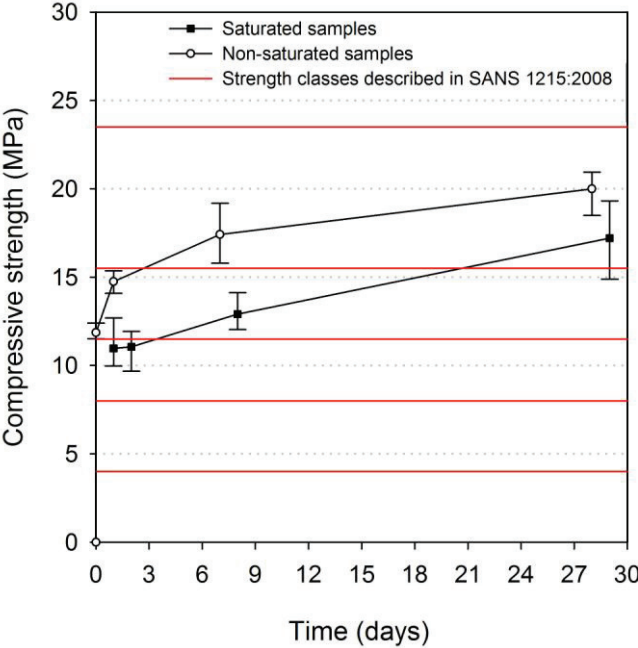
The weight loss from the interlayer and structurally bound water in the alkali aluminosilicate gel was lower in the outer-core than in the inner-core and both oven-cured samples, implying that the formation of the alkali aluminosilicate gel in the outer-core underwent a lower degree of reaction [26]. Nedeljković et al. (2016) [27] observed a relation between weight loss from TGA and the amorphous phase content of alkali-activated fly ash mixtures: an increase in amorphous content coincided with an increase in weight loss. A sample with a higher content of alkali aluminosilicate gel has a higher proportion of interlayer and structurally bound water weight loss from TGA than a sample with a lower content of alkali aluminosilicate gel.

At 1 day, the weight loss of both oven-cured samples and the inner-core of the confined-DEC sample were approximately similar, as were the amorphous phase contents (Table 3), within the margin of error. The relation between weight loss and amorphous phase content therefore holds true in this case [27]. The amorphous phase content of the outer-core was also similar to that of the other samples at day 1, within the margin of error (Table 3), but the weight loss of the outer-core sample was considerably less than that of other samples (Fig. 6). This

contradicts Nedeljković et al.'s (2016) [27] observation. Otherwise, the weight loss of the outer-core would have been similar to that of the other samples. However, the egress of Na^+ and OH^- ions from the outer-core during confined-DEC explains this contradiction. The outer-core showed an increase in amorphous phase content due to the reduction in NaOH and, to a lesser extent, due to the formation of alkali aluminosilicate gel.

3.5. Standard compliance

The samples prepared with confined-DEC were tested against the South African concrete masonry units' standard, SANS 1215:2008 [9]. For the compressive strength test, the standard requires samples to be saturated in water for 24 h before testing. The compressive strength development of saturated and non-saturated confined-DEC samples as well as the minimum compressive strength requirements of masonry units containing aggregates for different strength classes described in SANS 1215:2008 [9], are shown in Fig. 7.



(Single column, 90 mm, fitting image)

Fig. 7. Compressive strength development of saturated and non-saturated samples

According to the compressive strength requirements of the different strength classes of masonry units containing aggregates presented in Fig. 7, the confined-DEC samples right after curing (7 min) complied with the two lowest compressive strength classes, 4.0 and 8.0 MPa. At 28 days the confined-DEC samples met the requirements of the following compressive strength classes: 4.0, 8.0, 11.5 and 15.5 MPa.

The surface texture requirement states that the surface must provide adequate adhesion for the plaster or the finish. The confined-DEC samples failed to comply with this requirement due to the poorly developed outer-core. Drying shrinkage and re-welting on expansion compliance tests were therefore abandoned, since the tests relied on utilizing the surface of the samples. Thus, more research should be done in future to address the quality of surface layer of samples prepared with confined-DEC, with the aim to meet the requirements of the standard [9].

3.6. General remarks

The potential loss in compressive strength at later ages could impede the practical application of confined-DEC in the brick-making industry (Fig. 3). However, as long as sufficient compressive strength is obtained with respect to standard compliance, the confined-DEC still proved to be a better manufacturing alternative than oven curing. Duration of curing, reduced from 16 h to 7 min, can be considered as an acceptable trade-off in potential compressive strength loss from 32.2 to 20.5 MPa at 28 days. Considering that the energy input is more efficient with confined-DEC than with traditional elevated temperature curing methods [28; 29], the notable reduction in the duration of curing also significantly lowers energy consumption. Furthermore, Belden et al.'s (2012) [6] manufacturing approach of fly ash based bricks on an industrial scale consists of several stages (press moulding, drying and

firing), but confined-DEC consists of only one stage. Thus, the confined-DEC technique would simplify the manufacturing approach compared to conventional methods, which would reduce the total manufacturing time. Hence, confined-DEC is a promising approach in the rapid accelerated curing of NaOH-activated fly ash based brick mixtures as an alternative manufacturing method.

5. Conclusions

The loss in potential compressive strength gain at 28 days for the confined-DEC samples is attributable to the development of the outer-core and, to a lesser extent, that of the inner-core. Substantial evidence, gained from ATR-FTIR, XRD and TGA, indicates that the outer-core developed poorly in comparison to the inner-core; and, hence, the material was only as strong as its weakest part, namely the outer-core.

The prime cause for the loss in potential strength at 28 days of the confined-DEC samples was the decrease in Na₂O content from the diminishing pore solution. XRD, XRF and TGA confirmed the egress of Na⁺ and OH⁻ ions from the outer-core but did not support the egress of ions from the inner-core to the same degree as that from the outer-core. This loss in alkali content consequently affected the potential compressive strength at 28 days.

The confined-DEC samples failed to comply with the surface finish requirement of SANS 1215:2008. Nevertheless, the compressive strength requirements of several strength classes described in SANS 1215:2008 were met within 7 min after the application of the confined-DEC technique, and higher strength classes were satisfied at 28 days.

The confined-DEC technique is therefore a promising approach to the rapid accelerated curing of NaOH-activated fly ash based brick mixtures. The studied mixture, consisting of 4.1% NaOH flakes, 9% water and 86.9% fly ash by weight, gained a compressive strength of 11.5 MPa in 7 min and continued to increase in compressive strength to 20.1 MPa at 28 days.

The considerable decrease in the duration of curing from hours to minutes is desirable in the brick-making industry. However, the negative effect associated with confined-DEC under free drainage conditions, which was found during this investigation, should be addressed in future. Solving the problem of the diminishing pore solution would provide an attractive alternative for mass production of fly ash bricks and thus would increase the utilisation of fly ash and would provide an inexpensive building material.

6. Recommendations

To counteract the negative effect of the studied confined-DEC set-up, total confinement (un-drained conditions) of the NaOH-activated fly ash based brick mixture during curing can be applied. The pore solution will subsequently not have the possibility to diminish during curing and, therefore, the entire mixture will experience a sufficient curing environment without a decrease in Na_2O content. The total confinement of the mixture should consist of a two-stage process. The initial confinement of the mixture must occur under free drainage conditions so that the solid constituent, fly ash, carries the load and not the water; this will reduce porosity and improve the durability of the cured mixture. Finally, then only total confinement of the mixture should be applied before curing.

After the curing is complete, removing the cured mixture from the curing device should also consist of a two-stage process. Firstly, the un-drained conditions should be removed, but confinement under free drainage conditions must still be present. This will relieve the inner water pressure build-up within the mixture by allowing the water to escape into the drainage paths; steam will be observed emerging from the drainage paths. Secondly, after the steam has ceased, it will be possible to remove the cured mixture safely from the device. Otherwise, immediate removal of the cured mixture will result in the bursting of fragments of the cured mixture because of the high generated internal tensile stresses. Davidovits and Legrand

(1977) [5] observed the burst of fragments of the cured mixture after the immediate removal of total confinement. These authors counteracted this dilemma by providing a mechanism that relieved the water pressure build-up.

Another approach that can potentially counteract the observed problem without altering the current confined-DEC set-up, is the creation of un-drained conditions within the mixture. When saturated clay is put under a load, it will not release water immediately. This property of clay can be used by incorporating it into the NaOH-activated fly ash based brick mixture. Kumar and Ambarish (2013) [30] observed that the addition of at least 20% clay by weight to fly ash significantly decreased the hydraulic conductivity of the material. Mingyu et al. (2009) [31] synthesised an alkali-activated fly ash based mixture with bentonite and observed that the bentonite acted as a filler, making the material more compact.

Eliminating the effect of the diminishing pore solution during confined-DEC would create a possibility of applying extremely high heating rates through higher voltage gradients, which could decrease the curing duration to less than 1 min. Incorporating this concept into multi-cell moulds on highly automated production lines would provide an attractive alternative for high-volume fly ash utilisation.

7. References

[1] Eskom Integrated Report 2014. <http://integratedreport.eskom.co.za/pdf/full-integrated.pdf> (accessed 07.12.2015).

[2] 2012 National Development Plan 2030 Our future - make it work.

[http://www.poa.gov.za/news/Documents/NPC National Development Plan Vision 2030 -lo-res.pdf](http://www.poa.gov.za/news/Documents/NPC_National_Development_Plan_Vision_2030_-_lo-res.pdf), (accessed 07.12.2015)

[3] M. Ziolkowski, M. Kovtun, Confined-Direct Electric Curing of NaOH-activated fly ash brick mixtures under free drainage conditions: Part 1. Factorial experimental design, *Constr. Build. Mater.* 155C (2017) 1050-1062.

[4] R.T. Belden, M. Cristallo, G. Ittmann, R. Ittmann, Bricks and method of forming bricks with high coal ash content using a press mold machine and variable firing trays, US Patent 2012/0031306 A1, 2012.

[5] J. Davidovits, J.J. Legrand, Process for agglomerating compressible mineral substances under the form of powder, particles or fibres, US Patent 4028454, 1977.

[6] C. Ferone, F. Colangelo, R. Cioffi, F. Montagnaro, L. Santoro, Mechanical performances of weathered coal fly ash based geopolymer bricks, *Proc. Eng.* 21 (2011) 745–752,
<http://dx.doi.org/10.1016/j.proeng.2011.11.2073>

[7] M.B. Diop, M.W. Grutzeck, Low temperature process to create brick, *Constr. Build. Mater.* 22 (6) (2008) 1114–1121, <http://dx.doi.org/10.1016/j.conbuildmat.2007.03.004>

[8] G. Kovalchuk, A. Fernández-Jiménez, A. Palomo, Alkali-activated fly ash: Effect of thermal curing conditions on mechanical and microstructural development - Part II, *Fuel* 86 (3) (2007) 315-322.
<http://dx.doi.org/10.1016/j.fuel.2006.07.010>

[9] SANS 1215:2008. Concrete masonry units, Edition 1.4, Standards South Africa, Pretoria.

[10] J. C. Swanepoel, C. A. Strydom, Utilisation of fly ash in geopolymeric material, *Appl.*

Geochem. 17 (8) (2002) 1143-1148.

[https://doi.org/10.1016/S0883-2927\(02\)00005-7](https://doi.org/10.1016/S0883-2927(02)00005-7)

[11] J. Shekhovtsova, E.P. Kearsley, M. Kovtun, Effect of activator dosage, water-to-binder-solids ratio, temperature and duration of elevated temperature curing on the compressive strength of alkali-activated fly ash cement pastes, J. S. Afri. Inst. Civ. Eng. 56 (3) (2014) 44–52.

[12] A. Noushini, A. Castel, [The effect of heat-curing on transport properties of low-calcium fly ash-based geopolymer concrete](#), Constr. Build. Mater. 112 (2016) 464–477.

<https://doi.org/10.1016/j.conbuildmat.2016.02.210>

[13] E. Arioz, O. Arioz, O. M. Kockar, Leaching of F-type fly Ash Based Geopolymers, Procedia Eng. 42 (2012) 1114-1120.

<https://doi.org/10.1016/j.proeng.2012.07.503>

[14] J.G.S. van Jaarsveld, J.S.J. van Deventer, G. C. Lukey, The effect of composition and temperature on the properties of fly ash- and kaolinite-based geopolymers, Chem. Eng. J. 89 (1-3) (2002) 63-73.

[https://doi.org/10.1016/S1385-8947\(02\)00025-6](https://doi.org/10.1016/S1385-8947(02)00025-6)

[15] I. Ismail, S. A. Bernal, J. L. Provis, S. Hamdan, J. S. van Deventer, Drying-induced changes in the structure of alkali-activated pastes, J. Mater. Sci. 48 (9) (2013) 3566-3577.

<https://doi.org/10.1007/s10853-013-7152-9>

[16] [A. Fernández-Jiménez](#), A. Palomo, Composition and microstructure of alkali activated

fly ash binder: Effect of the activator, *Cem. Concr. Res.* 35 (10) (2005) 1984-1992.

[17] M. Criado, A. Fernández-Jiménez, A. Palomo, Alkali activation of fly ash: Effect of the SiO₂/Na₂O ratio: Part 1: FTIR study, *Microporous Mesoporous Mater.* 106 (1-3) (2007) 180-191.

<https://doi.org/10.1016/j.micromeso.2007.02.055>

X[18] M. Criado, [A. Fernández Jiménez](#), I. Sobrados, A. Palomo, J. Sanz, Effect of relative humidity on the reaction products of alkali activated fly ash, *J. Eur. Ceram. Soc.* 32 (11) (2012) 2799-2807.

<https://doi.org/10.1016/j.jeurceramsoc.2011.11.036>

[19] J. Shekhovtsova, Using South Africa fly ash as a component of alkali-activated binder, (2015) Ph.D thesis, University of Pretoria, South Africa.

[20] Y. Zhang, W. Sun, Z. Li, Preparation and microstructure characterization of poly-sialate-disiloxo type of geopolymeric cement, *J. Cent. South. Univ. Technol.* 16 (2009) 906-913.

<https://doi.org/10.1007/s11771-009-0151-y>

[21] W.K.W. Lee, J.S.J. Van Deventer, The effects of inorganic salt contamination on strength and durability of geopolymers, *Colloids Surf. A: Physicochem. Eng. Aspects* 211 (2-3) (2002) 115-126.

[https://doi.org/10.1016/S0927-7757\(02\)00239-X](https://doi.org/10.1016/S0927-7757(02)00239-X)

[22] Criado et al. (2005) M. Criado, A. Palomo, A. Fernández-Jiménez, Alkali activation of fly ashes. Part 1: Effect of curing conditions on the carbonation of the reaction products, *Fuel*,

84 (16) (2005) 2048-2054.

<https://doi.org/10.1016/j.fuel.2005.03.030>

[23] G. V. P. B. Singh, K. V. L. Subramaniam, Quantitative XRD study of amorphous phase in alkali activated low calcium siliceous fly ash, *Constr. Build. Mater.* 124 (2016) 139-147.

<https://doi.org/10.1016/j.conbuildmat.2016.07.081>

[24] J. Xie, O. Kayali, Effect of initial water content and curing moisture conditions on the development of fly ash-based geopolymers in heat and ambient temperature, *Constr. Build. Mater.* 67 (Part A) (2014) 20-28.

Mater. 67 (Part A) (2014) 20-28.

<https://doi.org/10.1016/j.conbuildmat.2013.10.047>

[25] S. Ahmari, L. Zhang, Production of eco-friendly bricks from copper mine tailings through geopolymerization, *Constr. Build. Mater.* 29 (2013) 323–331.

<http://dx.doi.org/10.1016/j.conbuildmat.2011.10.048>

[26] S. Shi, H. Li, M. Fabian, T. Sun, K. T. V. Grattan, D. Xu, P. A. M. Basheer, Y. Bai, Alkali-Activated Fly Ash Manufactured with Multi-stage Microwave Curing, Fourth International Conference on Sustainable Construction Materials and Technologies, Las Vegas, US (2016)

[27] Nedeljković et al. (2016) M. Nedeljković, K. Arbi, Y. Zuo, G. Ye, Microstructural and Mineralogical Analysis of Alkali Activated Fly Ash-Slag Pastes, 3rd International RILEM Conference on Microstructure Related Durability of Cementitious (2016) 1-10.

[28] I.D. Kafry, *Direct Electric Curing of Concrete: Basic Design*, Whittles Publishing,

Latheronwheel, 1993.

[29] S.S. Wadhwa, L.K. Srivastava, D.K. Gautam, D. Chandra, Direct electric curing of in situ concrete, *Batim. Int. Buil. Res. Pract.* 15 (1–6) (1987) 97–101.

<http://dx.doi.org/10.1080/09613218708726799>

[30] S. K. Pal, A. Ghosh, Hydraulic Conductivity of Fly Ash-Montmorillonite Clay Mixtures, *Indian Geotech. J.* 43 (1) (2012) 47-61.

<https://doi.org/10.1007/s40098-012-0033-3>

[31] H. Mingyu, Z. Xiaomin, L. Fumei, Alkali-activated fly ash-based geopolymers with zeolite or betonite as additives, *Cem. Con. Compost.* 31 (10) (2009) 762-768.

<https://doi.org/10.1016/j.cemconcomp.2009.07.006>